P_3 are 2·0, 4·0, and 0·0. In pyrite, the distorted octahedral field may be expected to favor the population of the a_g orbital over the e_g orbitals since the S–Fe–S angle of 94·3° is greater than 90° for S atoms related by the threefold axis, thus increasing the mean distance between the ligands and electrons in the a_g orbital. This effect is indeed found to be significant. Both refinements (II) and (III) show considerable distortion from a spherical charge distribution towards the low-spin configuration with preference for population of the a_g orbital. The refined values of ζ, 3·79–3·93 a.u.$^{-1}$, correspond to a slightly contracted 3*d* shell compared with the optimized single Slater exponent of 3·73 a.u.$^{-1}$ calculated for an isolated iron atom by Clementi & Raimondi (1963).

The experimental deformation density about iron is plotted in Fig. 1 along with a plot of the model density corresponding to the parameters obtained from refinement (III). Both maps have been calculated including X-ray measurements with $I > 3\sigma(I)$ and include the smearing due to thermal motion of the atoms.

Rees & Mitschler (1976) have estimated the relative occupancies of the t_{2g} and e_g orbitals in the octahedral complex $Cr(CO)_6$ from the observed differences in the experimental density along the octahedral threefold and fourfold axes. Iwata (1977) has refined the populations of the a_g, e_g and e'_g orbitals using X-ray data from two compounds containing the nearly octahedral complexes, $[Co(NH_3)_6]$ and $[Co(NH_3)_6][Co(CN)_6]$. Her refinements, however, included only a portion of the X-ray data with all other parameters including the radial dependence of the density functions fixed.

Conclusion

With the expressions described here, orbital occupancies and estimated standard deviations can readily be obtained using existing aspherical refinement programs. Following the same approach, similar expressions can be derived from other site symmetries. This method can be expected to be useful as long as the effects of the crystal environment about the metal atom are primarily electrostatic and the covalent interactions are minor. A further limitation is imposed by the restricted form of the radial functions used in the analysis.

Support of this work by the National Science Foundation and by the donors of the Petroleum Research Fund administered by the American Chemical Society is gratefully acknowledged.

References

BALLHAUSEN, C. J. (1962). *Introduction To Ligand Field Theory*, p. 68. New York: McGraw-Hill.
CLEMENTI, E. & RAIMONDI, D. L. (1963). *J. Chem. Phys.* **38**, 2686–2689.
COPPENS, P., GURU ROW, T. N., LEUNG, P., STEVENS, E. D., BECKER, P. J. & YANG, Y. W. (1979). *Acta Cryst.* A**35**, 63–72.
HANSEN, N. K. & COPPENS, P. (1978). *Acta Cryst.* A**34**, 909–921.
HAREL, M. & HIRSHFELD, F. L. (1975). *Acta Cryst.* B**31**, 162–172.
IWATA, M. (1977). *Acta Cryst.* B**33**, 59–69.
IWATA, M. & SAITO, Y. (1973). *Acta Cryst.* B**29**, 822–832.
JOHNSON, C. K. (1969). *Acta Cryst.* A**25**, 187–194.
MARUMO, F., ISOBE, M., SAITO, Y., YAGI, T. & AKIMOTO, S. (1974). *Acta Cryst.* B**30**, 1904–1906.
RAE, A. D. (1978). *Acta Cryst.* A**34**, 719–724.
REES, B. & MITSCHLER, A. (1976). *J. Am. Chem. Soc.* **98**, 7918–7924.
ROSE, M. E. (1957). *Elementary Theory of Angular Momentum*, p. 61. New York: Wiley & Sons.
STEVENS, E. D., DELUCIA, M. L. & COPPENS, P. (1979). In preparation.
STEWART, R. F. (1976). *Acta Cryst.* A**32**, 565–574.
VICAT, J., TRANQUI, D. & ALEONARD, S. (1977). *Acta Cryst.* B**33**, 1180–1190.
WANG, Y. & COPPENS, P. (1976). *Inorg. Chem.* **15**, 1122–1127.

Acta Cryst. (1979). A**35**, 539–543

A Discussion on Constrained Refinements

BY RICCARDO BIANCHI, RICCARDO DESTRO, TULLIO PILATI AND MASSIMO SIMONETTA
Istituto di Chimica Fisica e Centro CNR, Università, via Golgi 19, 20133 *Milano, Italy*

(*Received* 17 *October* 1978; *accepted* 13 *February* 1979)

Abstract

Three crystal structures are discussed in order to emphasize the difference between statistical and chemical or physical grounds of the different models used to represent crystal structure. The constrained models give an evident improvement over the unconstrained models for disordered crystal structures; they can also explain anomalies resulting at the end of the conventional refinement.

0567-7394/79/040539-05$01.00

Introduction

In the present study a specific analysis of three crystal structures is made, utilizing models which impose particular relationships between the atomic parameters. The purpose of this investigation is to re-examine the unconstrained model in such a way as to stress the differences between the various models used to describe crystal structure, in the comparison between statistical grounds and chemical or physical grounds. In fact, there are cases in which the unconstrained model, even if more significant from the statistical point of view, is chemically or physically equivalent to the constrained model (see for example Bianchi, Destro & Simonetta, 1979).

For this work we have selected three structures, whose data were collected at low temperature, which present at the end of the conventional refinement three different problems. For each structure, a description of the problem is given together with all tests on various constrained models.

DIF

The structure of 11,11-difluoro-1,6-methano[10]-annulene (DIF) was determined at room temperature (Gramaccioli & Simonetta, 1971) and at 173 K (Pilati & Simonetta, 1976).

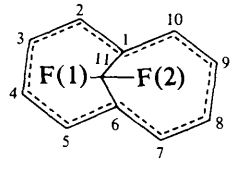

Crystal data at 173 K were $a = 9{\cdot}111\ (1)$, $b = 13{\cdot}203\ (2)$, $c = 6{\cdot}981\ (1)$ Å, $Z = 4$; orthorhombic, space group $Pna2_1$.

The molecular geometry obtained by analysis of room-temperature data shows an unexpected distortion from free-state molecular symmetry. The molecular model derived from X-ray data collected at low temperature is near to C_2 symmetry: all the differences from C_2 symmetry are within three times the standard deviation, except for the angles C(6)–C(11)–F(1), 114·0 (2)° and the C_2 symmetry related C(1)–C(11)–F(2), 113·0 (2)°; the discrepancy from *mm*2 symmetry is more marked. On the basis of these considerations four constrained refinements were carried out for 873 reflections with $F^2 > 2\sigma(F^2)$. The results for the models tried are reported in Tables 1 and 2.

The fluorine and hydrogen atoms were excluded from **TLS** constraint in models (I), (II) and (III).

As a test for significance we use that proposed by Hamilton (1965). The ratio

$$\mathscr{R}_{obs} = \left\{ \frac{R_w(\mathrm{I})}{R_w(\mathrm{II})} \right\}^{1/2}$$

is calculated and compared with the statistical distribution of $\mathscr{R}$. The percentage points of the $\mathscr{R}$ distribution are calculated for the degrees of freedom appropriate to our problem by the method of Pawley (1970).

The program used for constrained refinements was recently written by Bianchi, Pilati & Simonetta (1978).

Examining the value of $\mathscr{R}_{obs}$ for the compared models (I)/(V) (see Table 2), we deduce that model (I) is strongly rejected by Hamilton's test. Indeed, the difference Fourier map of model (I) has residuals of electron density of around 0·30 e Å^{-3} in the zone of the fluorine atoms; while in that of the unconstrained model they are about 0·10 e Å^{-3}. The shortest intermolecular distances are similar in both models but with a little shortening for model (I), for example the contact F(2)···H(4) is 2·541 and 2·498 Å for unconstrained and constrained models respectively.

As regards the other models (II), (III) and (IV), we deduce again a statistical worsening of the agreement between observed and calculated structure factors (see Table 2); this seems to indicate that the constraints are not supported by the data. However, it is to be underlined that the difference Fourier maps, the geometries and the shortest intermolecular contacts, obtained from models (II), (III) and (IV) are equivalent (within the experimental uncertainties) to those derived from model (V). Therefore we conclude that the constrained models

Table 1. *Agreement factors of least-squares refinements for DIF*

Model	Constraints	R%*	R_w%†
(I)	*mm*2 molecular symmetry + **TLS**	4·93	4·87
(II)	2 molecular symmetry + **TLS**	4·57	4·37
(III)	**TLS**	4·32	4·10
(IV)	2 molecular symmetry	4·29	4·02
(V)	unconstrained	4·02	3·73

* $R = \sum||F_o| - |F_c||/\sum|F_o|$.
† $R_w = [\sum w(|F_o| - |F_c|)^2/\sum w(F_o)^2]^{1/2}$; $w = 1/\sigma^2(F_o)$.

Table 2. *Percentage points of the $\mathscr{R}$ distribution for comparing the DIF models*

N_c and N_{unc} are the number of parameters used in the constrained and unconstrained models respectively. The number of observations is 873 in all cases.

Models compared	$\mathscr{R}_{obs}$	N_c	N_{unc}	Probability levels of $\mathscr{R}$ distribution 0·25	0·01	0·001
(I)/(V)	1·142	61	149	1·065	1·083	1·092
(II)/(V)	1·083	75	149	1·055	1·072	1·080
(III)/(V)	1·048	103	149	1·036	1·049	1·056
(IV)/(V)	1·038	121	149	1·022	1·033	1·039

(II), (III) and (IV) have chemical or physical grounds comparable with those of model (V) to describe the crystal structure of DIF; even if the unconstrained model is preferred at 99% significance level.

DINO

The crystal structure of *sym*-dibenzo-1,5-cycloocta-diene-3,7-diyne (DINO) was determined at 290, 218 and 113 K (Destro, Pilati & Simonetta, 1977). The crystal data at 113 K were $a = 6{\cdot}0388\ (12)$, $b = 11{\cdot}8041\ (18)$, $c = 13{\cdot}9163\ (24)$ Å, $Z = 4$; monoclinic, space group $P2_1/n$.

At 113 K the structural parameters determined by the conventional refinement define a molecular symmetry near to *mm*2. However, the parameter differences between the *mm*2 case and the situation as obtained from the usual refinement are up to three times the standard deviation.

The errors in the electron-density residues, derived from estimated σ's of the observed data (Cruickshank, 1949) is 0·04 e Å^{-3}. Furthermore, the difference Fourier map reveals an interesting feature in the planes of the benzene rings and particularly in the region close to the triple bonds. In fact, the distribution of electron density around the triple bonds is asymmetric with a slight accumulation of charge inside the central eight-membered ring, and along the triple bonds there are holes of electron density (see Fig. 1*a* and *b*). This characteristic was also found by Irngartinger, Leiserowitz & Schmidt (1970) in the room-temperature averaged electron density distribution of a molecule which consists of a three identical $-C_6H_4-C{\equiv}C-$ subunits, 1:2,5:6,9:10-tribenzocyclododeca-1,5,9-triene-3,7,11-triyne. These authors assert that the above mentioned effects are due to 'errors inherent in the determination of atomic thermal parameters from room-temperature X-ray data up to the usual sin θ/λ limit of 0·66 Å^{-1}'. On the other hand, this interpretation is not convincing since the deep negative residues are also found in the low-temperature difference map (Destro, Pilati & Simonetta, 1977).

In order to obtain an explanation, four constrained refinements were carried out with 2138 reflections collected at 113 K. The results are reported in Tables 3 and 4. The values of $\mathcal{R}_{obs}$ in Table 4 indicate that the unconstrained model (V) is statistically preferred, while the comparison between the constrained models shows that the model with **TLS** constraint is the most probable. Moreover, in the difference density map derived from **TLS** constraint, the holes of electron density along the triple bonds have disappeared (see Fig. 1*c* and *d*) and in the middle of the triple bonds the residual values are about 0·04 e Å^{-3}, as is expected. This proves the chemical improvement of model (III) with respect to model (V).

BDP

The crystal structure of bicyclo[5.4.1]dodeca-pentaenylium hexafluorophosphate (BDP) was determined at 110 K (Destro, Pilati & Simonetta, 1976). Crystal data were $a = 15{\cdot}478\ (4)$, $b = 6{\cdot}821\ (2)$, $c = 11{\cdot}373\ (3)$ Å, $Z = 4$; orthorhombic, space group *Pcam*.

In this case the cation is disordered so that the observed electron density is a 1:1 superposition of two annulene systems with their seven- and eight-membered rings interchanged.

The full-matrix least-squares refinement, using anisotropic temperature factors for P and F atoms, and isotropic temperature factors for the cation atoms, led to $R = 0{\cdot}076$ and $R_w = 0{\cdot}072$, goodness of fit 1·96 for 85 independent parameters and 2278 observed reflections.

The final difference density map has peaks slightly greater than 0·70 e Å^{-3} in the proximity of the cation. Sections of the ΔF syntheses through the annulene system are represented in Fig. 2(*a*).

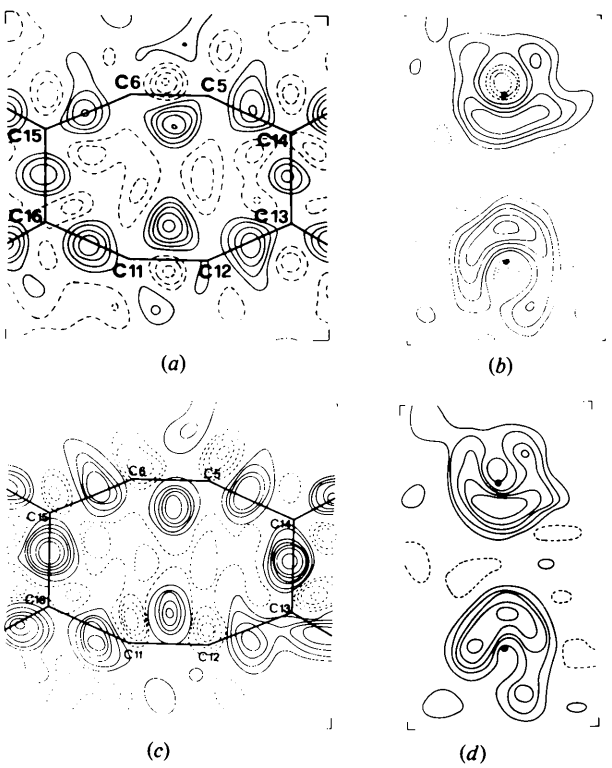

Fig. 1. (*a*) Section of the ΔF syntheses for DINO derived from model (V) showing residual electron density on the plane through the triple bonds. Contour levels at intervals of 0·05 e Å^{-3}; solid lines positive, dashed lines negative, zero contours omitted. (*b*) Difference-density section perpendicular to the triple bonds at their centres. Contours as in (*a*). The centres of the triple bonds are represented by the shaded circles. (*c*) As in (*a*) for model (III). (*d*) As in (*b*) for model III.

Table 3. *Agreement factors of least-squares refinements for DINO*

Model	Constraints	R%	R_w%
(I)	*mm*2 molecular symmetry + **TLS**	5·56	6·11
(II)	2 molecular symmetry + **TLS**	5·26	5·75
(III)	**TLS**	4·96	5·39
(IV)	2 molecular symmetry	4·81	5·23
(V)	unconstrained	4·56	4·63

Table 4. *Percentage points of the $\mathscr{R}$ distribution for comparing the DINO models*

N_c and N_{unc} are the number of parameters used in the constrained and unconstrained models respectively. The number of observations is 2138 in all cases.

Models compared	$\mathscr{R}_{obs}$	N_c	N_{unc}	Probability levels of $\mathscr{R}$ distribution 0·25	0·01	0·001
(I)/(II)	1·031	51	70	1·005	1·009	1·011
(I)/(III)	1·065	51	102	1·014	1·019	1·022
(I)/(IV)	1·081	51	146	1·026	1·032	1·036
(I)/(V)	1·149	51	178	1·035	1·042	1·046
(II)/(III)	1·033	70	102	1·009	1·013	1·015
(II)/(IV)	1·049	70	146	1·021	1·027	1·030
(II)/(V)	1·114	70	178	1·030	1·037	1·040
(III)/(IV)	1·015	102	146	1·012	1·017	1·020
(III)/(V)	1·079	102	178	1·021	1·027	1·030
(IV)/(V)	1·063	146	178	1·009	1·014	1·016

Another refinement, using anisotropic temperature factors for P, F and C atoms, and isotropic B's for H atoms, gave lower R and R_w factors, but the cation geometry was unrealistic and the correlation coefficients between the structural parameters were very high (up to 0·71).

To obtain a more significant fit of the data, a constrained refinement was carried out assuming (i) $4/mmm$ molecular symmetry and **TLS** constraints for the anion PF_6^-, (ii) m molecular symmetry and **TLS** constraints for the disordered cation. The resulting R and R_w based on 70 independent parameters were respectively 0·066 and 0·060; the goodness of fit was 1·62. The final difference map has a maximum residual of 0·56 e Å^{-3} in the cation vicinity (see Fig. 2*b*).

Conclusions

From the three discussed examples, we deduce that the use of various kinds of constraints on structural parameters, apart from the evident improvement in the case of disordered structures (here BDP), can be useful in interpreting anomalies resulting at the end of the conventional refinement. (In the case of DINO it explains the troughs along the triple bonds.) The view seems to be that even when a constrained refinement should be rejected on statistical grounds, it may well be acceptable on chemical or physical grounds. It then follows that if the constraint is chemically or physically acceptable, the other parameters in the refinement will take on more meaningful values, giving rise to improvements such as in Fig. 1.

It is also interesting to compare the level of significance of the distortion found here for DIF and DINO with that found in other molecular structures. Pawley (1971) has suggested that

$$\mathscr{S} = \frac{\mathscr{R}_{obs} - 1}{\mathscr{R}(0{\cdot}01) - 1}$$

be calculated and used as a comparison between the results of similar constrained refinements on different

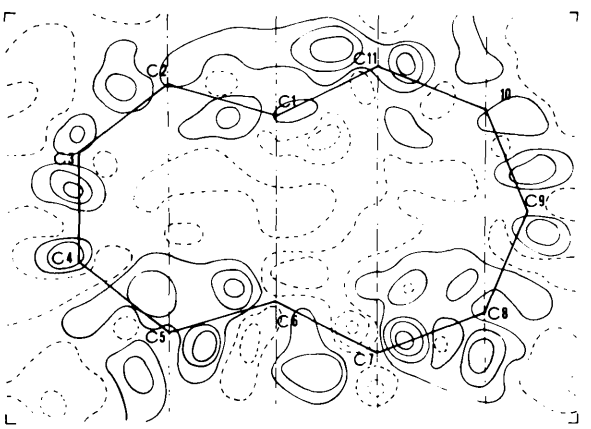

(*a*)

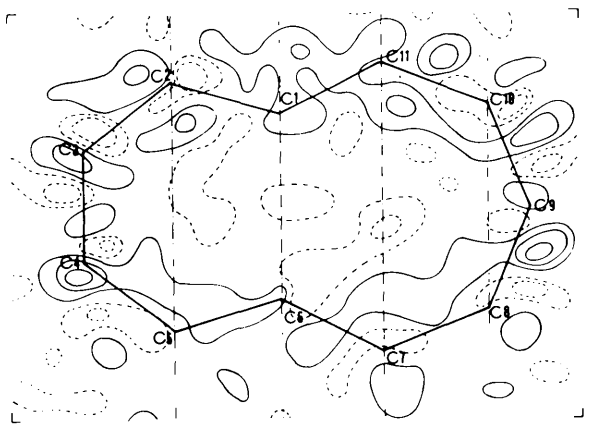

(*b*)

Fig. 2. Sections of the ΔF syntheses for BDP. Contour levels at intervals of 0·2 e Å^{-3}; solid lines positive, dashed lines negative; the first positive level is 0·10 e Å^{-3}. (*a*) Unconstrained model; the five sections are separated by chain-dotted lines and defined by the planes through atoms C(2), C(3), C(4), C(5); C(1), C(2), C(5), C(6); C(1), C(6), C(7), C(11); C(7), C(8), C(10), C(11); C(8), C(9), C(10). (*b*) As in (*a*) for the constrained model.

structures. For this comparison we have reported in Table 5 the $\mathscr{S}$ values of several structures. We note that the level of distortion of DIF is greater only than naphthalene; while that of DINO is near to anthracene and pyrene.

Table 5. *Comparison of the level of significance of the distortion among different structures*

Structure	$\mathscr{R}_{obs}$	$\mathscr{R}$ (0·01)	$\mathscr{S}$
DIF	1·142	1·083	1·7
DINO	1·149	1·042	3·5
S_8	1·154	1·015	10·3
Anthracene	1·092	1·023	4·0
Naphthalene	1·079	1·062	1·3
Pyrene	1·184	1·047	3·9
Ovalene	1·141	1·021	6·7
1,2,3-trichlorobenzene	1·070	1·038	1·8

References

BIANCHI, R., DESTRO, R. & SIMONETTA, M. (1979). *Acta Cryst.* B35, 1002–1005.

BIANCHI, R., PILATI, T. & SIMONETTA, M. (1978). *Comput. Chem.* 2, 49–51.

CRUICKSHANK, D. W. J. (1949). *Acta Cryst.* 2, 65–82.

DESTRO, R., PILATI, T. & SIMONETTA, M. (1976). *J. Am. Chem. Soc.* 98, 1999–2000.

DESTRO, R., PILATI, T. & SIMONETTA, M. (1977). *Acta Cryst.* B33, 447–456.

GRAMACCIOLI, C. M. & SIMONETTA, M. (1971). *Acta Cryst.* B27, 2231–2237.

HAMILTON, W. C. (1965). *Acta Cryst.* 18, 502–510.

IRNGARTINGER, H., LEISEROWITZ, L. & SCHMIDT, G. M. J. (1970). *J. Chem. Soc. B*, pp. 497–504.

PAWLEY, G. S. (1970). *Acta Cryst.* A26, 691–692.

PAWLEY, G. S. (1971). *Advances in Structure Research by Diffraction Methods*, Vol. 4. Edited by W. HOPPE & R. MASON, p. 62. Oxford: Pergamon Press.

PILATI, T. & SIMONETTA, M. (1976). *Acta Cryst.* B32, 1912–1913.

Acta Cryst. (1979). A35, 543–547

The Number of Permitted Modes of Propagation in *N*-Beam Dynamical Diffraction of X-rays

BY SHIH-LIN CHANG

Instituto de Física 'Gleb Wataghin', Universidade Estadual de Campinas, 13100 *Campinas, São Paulo, Brasil*

(*Received* 6 *October* 1978; *accepted* 16 *January* 1979)

Abstract

It is shown that the real part of the root of the dispersion equation for the permitted modes of propagation is always positive for two-beam Laue and Bragg reflections at the exact diffraction position. Based on this, a general rule is proposed to determine the number, N_p, of permitted modes of propagation for N-beam dynamical diffraction, where no extremely asymmetric reflections are involved. In other words, for both σ- and π-polarized wavefields,

$$N_p = 2(N - N_{\text{Bragg}}),$$

where N_{Bragg} is the number of Bragg reflections involved. This conclusion is supported by calculations for three-, four-, six- and eight-beam cases.

I. Introduction

In the dynamical theory of diffraction, the dispersion surfaces, amplitude ratios of wavefields and absorption coefficients are determined from the equation of dispersion. Each dispersion surface specifies a type of wave propagating through a crystal, the so-called mode of propagation. The wavefield and absorption coefficient are associated with their corresponding mode of propagation. The number of modes equals the number of existing wavefields. Other quantities such as the excitation of mode and diffracted intensities are obtained by combining the number of wavefields with the appropriate boundary conditions. Therefore, it is necessary to take the number of wavefields, namely, the number of permitted modes into account in dynamical calculations and only then comparison of the calculations with experiments can be made.

It has been well established that there are four permitted modes of propagation for two-beam (Laue) transmission of X-rays if both σ- and π-polarized wavefields are considered. However, according to Kohler (1933) and Authier (1962), there are only two modes allowed in two-beam symmetric Bragg reflection for a thick crystal, *i.e.* $\mu t > 10$, where μ and t are the linear absorption coefficient and the crystal thickness, respectively. These two modes, which have the direction of energy flow towards the crystal, are associated with

0567-7394/79/040543-05$01.00